PHYSICAL REVIEW B VOLUME 14, NUMBER 5 1 SEPTEMBER 1976

Magnetic ordering and domain-wall relaxation in zinc-ferrous ferrites

C. M. Srivastava, S. N. Shringi, R. G. Srivastava, and N. G. Nanadikar
Department of Physics, Indian Institute of Technology, Powai, Bombay 400076, India
(Received 5 August 1975)

The magnetic data and permeability spectra of the $Zn_xFe_{3-x}O_4$ system have been obtained for $x = 0$, 0.2, 0.4, 0.6, and 0.8. The observations indicate existence of a Yafet-Kittel type of magnetic ordering in the mixed ferrites. The permeability spectra have been analyzed in terms of processes involving domain-wall translation and domain rotation. The analysis shows that the ratio of the resonance frequency to the relaxation frequency for domain translation decreases monotonically as the zinc concentration is increased.

I. INTRODUCTION

Ferrous zinc ferrites have appreciably higher saturation magnetization compared to NiZn and MnZn ferrites and can be used with advantage in several applications where high values of $4\pi M_s$ are required. However because of preparation difficulties these have not so far been commercially exploited. This probably also explains the fact that only a few data on these ferrites are available in literature.[1-3] A successful method for synthesizing these materials in large quantities in a powder form was developed by Stuijts *et al.*[4] using a technique which required a low oxygen partial pressure. Appropriate proportions of powders were mixed by them and fired first for about 2 h at 1240 °C then at 1100 °C for 16 h in pure nitrogen atmosphere. Chemical analysis showed that the Fe^{2+} content was correct within 2 wt%. Magnetic measurements on these samples showed that the magnetization varied with zinc concentration and temperature in a similar manner as in other zinc substituted ferrites. Another method used by Dobson *et al.*[5] consisted of heating an appropriate mixture of the powder in evacuated sealed tubes at 950 °C for 7 h. However pellets prepared by them in a similar manner attained only 65% of the x-ray density and hence the method was not suitable for controlling the densification process. Moreover, the estimated ratio of Fe^{2+} to Zn in some samples was significantly different from the theoretical value. Mössbauer studies along with electrical-conductivity measurements were carried out by Dobson *et al.*[5] to investigate the charge transfer process in these materials. On account of the low density of the pellets which were used for the measurement of the electrical conductivity, they could not arrive at any meaningful and unambiguous conclusion regarding the mechanism of charge transfer. A detailed discussion of their analysis of the Mössbauer spectra is given in the following paper[6] (hereafter referred to as II).

We have used the method of Stuijts *et al.*[4] with slight modifications to prepare large quantities of these ferrites in pellet form with densities exceeding 90% of the x-ray densities. The compositions $Zn_xFe_{3-x}O_4$ with $x = 0$, 0.2, 0.4, 0.6, and 0.8 were obtained. Our measurements of the saturation magnetization show the same variation with zinc concentration and temperature as observed by Stuijts *et al.*[4] The variation of the magneton number n_B with zinc concentration in this system is similar in nature to that in the NiZn ferrite system and existence of Yafet-Kittel (YK) angles on the B site, observed in the latter case,[7] is strongly suspected. A molecular-field analysis of the YK spin ordering using the three-sublattice model is shown to explain the experimental data satisfactorily.

Mössbauer studies on $Zn_xFe_{3-x}O_4$ have been made at 77 and 300 °K. The room-temperature spectra are found to be similar in nature to those reparted by Dobson *et al.*[5] and are discussed in II. With large values of zinc concentration the spectra show relaxation effects at values of T/T_c much less than 1. Such effects have also been observed in other zinc substituted ferrites, e.g., LiZn,[8] CoZn,[9] and NiZn.[10] In a magnetically ordered phase the occurrence of such relaxation effects at temperatures significantly lower than the Néel temperature has not been satisfactorily explained. It will be shown in II that domain-wall relaxation processes are responsible for the observed Mössbauer line shapes in these cases. In this paper we report our analysis of the observed magnetization and permeability spectra, and in II we will discuss the correlation between magnetic and Mössbauer relaxation processes.

II. EXPERIMENTAL

The specimens were prepared with analytical reagent grade $\alpha - Fe_2O_3$ (USSR) and ZnO (Merck) in proper proportions to yield the desired composition on reduction. The powders were mixed in a steel-ball mill along with methanol for 12 h.

The mixed powders were dried and pressed into disk-shaped pellets of diameter 17 mm and 5 mm thickness at a pressure of 10 tons/in.^{2} The pellets were stacked on platinum boats and placed in the alumina tube of a horizontal silicon carbide furnace. Gas-tight tubular connections at the inlet and outlet of the alumina tube were provided to allow continuous flow of pure nitrogen during sintering. A small fraction of the inlet and the outlet gas was alternately made to flow through a zirconia cell to measure the oxygen content of the gas (Fig. 1). The temperature of the furnace was gradually raised to 1250 °C in about 8 h. Above this temperature, the oxygen content of the outgoing gas was found to increase. The temperature was raised till there was no further increase in the rate of evolution of oxygen. This generally occurred between 1250 and 1350 °C. The temperature was held constant at this particular value until the oxygen contents of the incoming and outgoing gases became equal. It was then lowered to 1100 °C and held at this temperature for 16 h to homogenize the ferrite. To prevent reoxidation the furnace was allowed to cool in stationary nitrogen atmosphere.

All the samples were found to be single-phase spinel by x-ray powder diffractometry. The lattice constants have been determined using Mo $K\alpha$ radiation and are given in Table I. Chemical analysis showed that the deviation of Fe^{2+} from the calculated value was within 2 wt% (see Table I).

The variation of the magnetization with temperature studied from 77 °K to the Néel temperature at a constant magnetic field of 7 kOe is shown in Fig. 2. The calculated values of the magneton number are given in Table II. These results are in broad agreement with those of Stuijts *et al.*[4] but there are some differences. The Néel temperatures for all the compositions are significantly higher than those reported by them though the values of magnetization at 77 and 300 °K in the two cases do not differ by more than 2%.

The permeability spectrum was obtained using

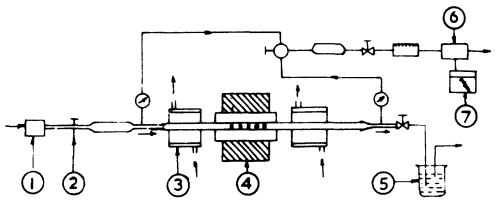

1. Purification of N_2
2. Vacuum pump
3. Water cooled joints
4. Closed furnace tube
5. Water seal
6. Zirconia element
7. Recorder

FIG. 1. Schematic diagram of the furnace assembly for sintering in gases with low oxygen content. Gas-tight tubular connections at the inlet and outlet of the alumina tube are provided to allow continuous flow of pure nitrogen during sintering. A small fraction of the inlet and the outlet gas is made alternately to flow through the zirconia cell to measure the oxygen content of the gas.

a rf admittance bridge (Model 33A/1, Boonton Electronic Corp.) and a coaxial line test set up (75 Ω). The complex permeability was measured at room temperature in the frequency range of 1–1000 MHz. The results are shown in Fig. 3.

III. ANALYSIS AND DISCUSSION

A. Lattice constant

The variation of lattice constant with zinc concentration is shown in Fig. 4 and is compared with the results of Miyata[3] (obtained using single crystals of $Zn_xFe_{3-x}O_4$). The agreement is fairly good. The increase in lattice constant with increasing zinc concentration is similar in nature to that in the NiZn ferrite[7] system and is due to the larger ionic crystal radius of Zn^{++} (0.74 Å) which on substitution replaces Fe^{3+} (0.60 Å) ion on the A site.

B. Magnetization

The magneton number n_B at 77 and 303 °K has been found initially to increase and then to decrease with increase in x as observed by Stuijts

TABLE I. Amount of Fe^{2+} present, from chemical analysis and calculated from formula, the lattice constant, and bulk density for different values of x for $Zn_x Fe_{3-x} O_4$.

x	Fe^{2+} content (wt%) Anal	Calc.	Lattice constant (Å)	Bulk density (g/cm^3)	Percentage of x-ray density
0.0	23.64	24.12	8.390	4.8	92.1
0.2	18.76	19.13	8.399	4.9	93.6
0.4	14.20	14.47	8.410	4.9	93.2
0.6	9.40	9.41	8.421	5.0	94.6
0.8	4.59	4.67	8.429	5.0	94.3

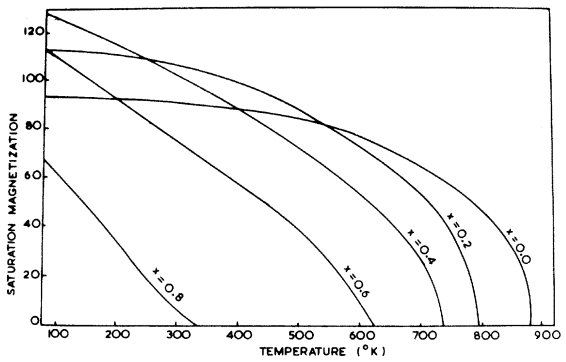

FIG. 2. Saturation magnetization (emu/g) as a function of temperature for $Zn_x Fe_{3-x} O_4$ for $x = 0$, 0.2, 0.4, 0.6, and 0.8. The measurements have been made between 77 °K and Néel temperature at a constant field of 7 kOe.

et al. (Fig. 5). The general trend of magnetization-versus-temperature curves (Fig. 2) for all the samples also agrees with their observations. However, there are some differences which arise primarily from the fact that the Néel temperatures for our samples are higher than those reported by Stuijts *et al.* (Table II). In some case, like for example $x = 0.6$, this difference is as large as 92 °C.

A similar variation of n_B with x has been observed also[11] in other Zn substituted ferrites like NiZn, CoZn, and MnZn. The variation in the NiZn ferrite was thought earlier to arise due to the presence of superparamagnetic clusters or paramagnetic centers formed due to insufficient magnetic linkages.[12] Recent neutron-diffraction measurements of Satya Murthy *et al.*[7] and low-temperature Mössbauer studies of Leung *et al.*[13] do not support this proposal. In the neutron-diffraction studies the paramagnetic scattering intensity was found to be much smaller than what would be expected on this model, while the Mössbauer spectra at 7 °K showed that every single composition between $x = 0$ to 1 was magnetically ordered and there was complete absence of a paramagnetic phase.

The ferromagnetic relaxation studies of the NiZn system have been made by Srivastava and Patni.[14] They observed that the ferromagnetic linewidth ΔH dropped first from about 600 Oe for $NiFe_2O_4$ to 150 Oe for $Ni_{0.8}Zn_{0.2}Fe_2O_4$ and then became almost independent of the zinc content. The presence of a paramagnetic phase acts as scattering center for spin waves from the uniform mode to the degenerate manifold and the linewidth is expected to increase approximately linearly with the increase in Zn content. Thus there is no experimental support for the cluster model from ferromagnetic relaxation data also.

It is now believed that the change in magnetization on zinc substitution occurs due to the presence of YK angles in the spin system on the B site as proposed by Satya Murthy *et al.*[7] on the basis of their neutron-diffraction measurements and later confirmed by a number of other workers.[10,13] On account of several similarities between the NiZn and the FeZn systems it is reasonable to assume that Yafet-Kittel angles are present in the latter system also. Our Mössbauer measurements presented in II support this spin ordering in the system.

The condition for the existence of YK angles in the NiZn system has been investigated in the molecular-field approximation by Satya Murthy *et al.*[7] using a noncollinear three sublattice model. In this model the molecular fields acting on various ions in the FeZn ferrites are given by

TABLE II. Saturation magnetization per formula unit in Bohr magnetons at 77 °K, the magnetization per gram at 303 °K, and the Néel temperature for $Zn_x Fe_{3-x} O_4$. For comparison the values of T_c obtained by Stuijts *et al.* (Ref. 4) are also given. The values of the exchange constants in °K used in calculating α_{YK} are as follows: $J_\alpha = -21$; $J_\beta = -28$; $J_\delta = -10$; $J_\gamma = -64$; $J_\epsilon = -24$.

x	n_B (77°K)	σ (emu/g) 303 °K	T_c (°K) Present work	T_c (°K) Stuijts *et al.*	α_{YK} (0 °K) Expt.	α_{YK} Calc.
0.0	3.9	91	875	838	0°	0°
0.2	4.7	108	788	763	14°4′	13°42′
0.4	5.4	100	732	695	24°29′	27°24′
0.6	4.8	71	624	532	41°24′	43°36′
0.8	2.9	6	335	•••	61°17′	63°18′

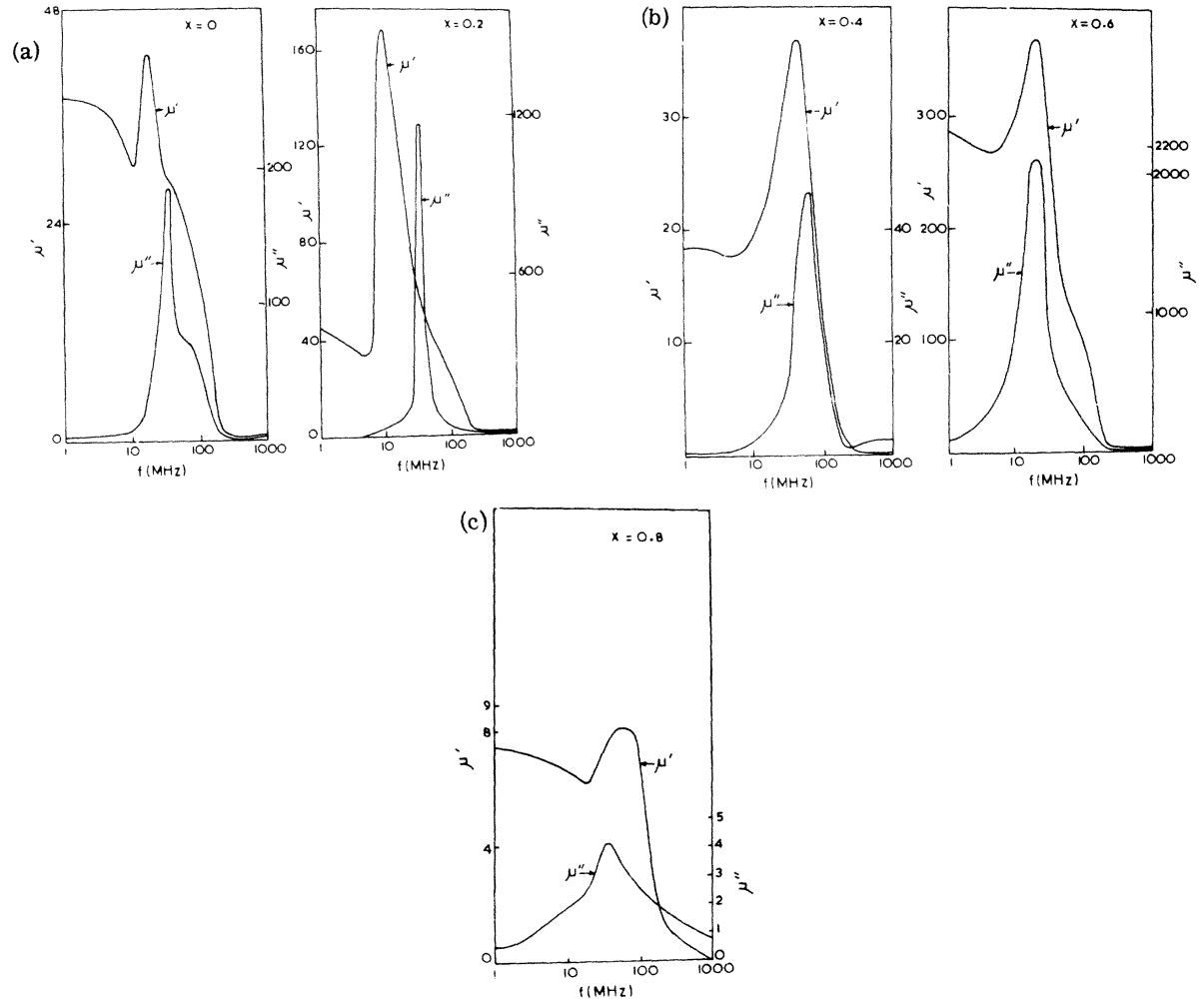

FIG. 3. Permeability spectrum of $Zn_xFe_{3-x}O_4$ at 300 °K for $x=0$, 0.2, 0.4, 0.6, and 0.8. The measurements up to 100 MHz were made using a rf admittance bridge and for higher frequencies a coaxial line (75 Ω) set up was used. The observed resonance in each case lies below the domain rotation and has been attributed to domain-wall oscillations. The broad resonance just after the sharp domain-wall resonance for $x=0$ is due to the dimensional effect.

$$\begin{bmatrix} \vec{H}_A(Fe^{3+}) \\ \vec{H}_{B_1}(Fe^{2+}) \\ \vec{H}_{B_1}(Fe^{3+}) \\ \vec{H}_{B_2}(Fe^{2+}) \\ \vec{H}_{B_2}(Fe^{3+}) \end{bmatrix} = \begin{bmatrix} \lambda_{AA} & \alpha & \beta & \alpha & \beta \\ \alpha & \gamma' & \epsilon' & \gamma & \epsilon \\ \beta & \epsilon' & \delta' & \epsilon & \delta \\ \alpha & \gamma & \epsilon & \gamma' & \epsilon' \\ \beta & \epsilon & \delta & \epsilon' & \delta' \end{bmatrix} \begin{bmatrix} (1-x)\vec{m}_A(Fe^{3+}) \\ \frac{1}{2}(1-x)\vec{m}_{B_1}(Fe^{2+}) \\ \frac{1}{2}(1+x)\vec{m}_{B_1}(Fe^{3+}) \\ \frac{1}{2}(1-x)\vec{m}_{B_2}(Fe^{2+}) \\ \frac{1}{2}(1+x)\vec{m}_{B_2}(Fe^{3+}) \end{bmatrix}, \tag{1a}$$

where

$$|\vec{m}_A(Fe^{3+})| = |\vec{m}_{B_1}(Fe^{3+})| = |\vec{m}_{B_2}(Fe^{3+})| = (N_A d/M)(5\mu_B),$$
$$|\vec{m}_{B_1}(Fe^{2+})| = |\vec{m}_{B_2}(Fe^{2+})| = (N_A d/M)(4\mu_B), \tag{1b}$$

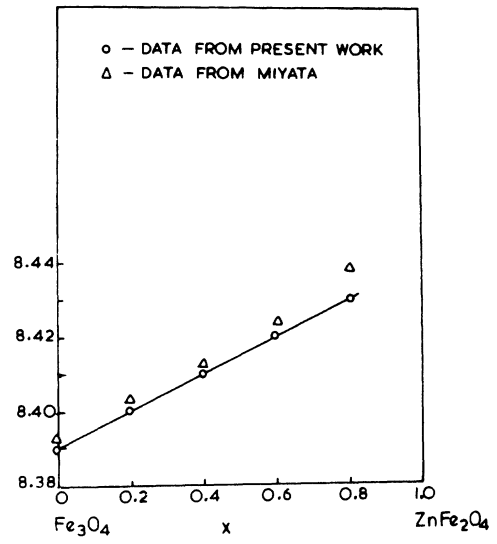

FIG. 4. Lattice constant in Å as a function of zinc content for $Zn_xFe_{3-x}O_4$. For comparison the data from Miyata (Ref. 3) has also been shown.

and N_A is the Avagadro's number, M and d are the molecular weight and density, respectively, of $Zn_xFe_{3-x}O_4$. The molecular-field constants relate to the following exchange interactions:

α: $A(Fe^{3+}) - B_i(Fe^{2+})$,

β: $A(Fe^{3+}) - B_i(Fe^{3+})$,

γ: $B_1(Fe^{2+}) - B_2(Fe^{2+})$,

γ': $B_i(Fe^{2+}) - B_i(Fe^{2+})$,

δ: $B_1(Fe^{3+}) - B_2(Fe^{3+})$,

δ': $B_i(Fe^{3+}) - B_i(Fe^{3+})$,

ϵ: $B_1(Fe^{3+}) - B_2(Fe^{2+})$,

ϵ': $B_i(Fe^{3+}) - B_i(Fe^{2+})$,

where $i = 1, 2$. We have, for example,

$$\alpha = 2z_{AB_i}J_\alpha/N_{B_i}g_A g_{B_i}\mu_B^2, \tag{1c}$$

where J_α is the interaction between $A(Fe^{3+})$ and $B_i(Fe^{2+})$. z_{AB_i} is the B_i nearest neighbors to A, N_{B_i} is the number of B_i ions per unit volume, μ_B is the Bohr magneton, and g denotes the Landé splitting factor. On physical grounds, we expect $J_\gamma, J_\delta, J_\epsilon$ to be close to $J_{\gamma'}$, $J_{\delta'}$, and $J_{\epsilon'}$, respectively, but they are not necessarily equal. This is so since $ZnFe_2O_4$ (for which only δ and δ' exist) is magnetically ordered at low temperatures and $\delta = \delta'$ is not permissible in this case. If Fe^{2+} and Fe^{3+} have moments of $4\mu_B$ and $5\mu_B$, respectively, it can be shown that YK ordering is possible provided

$$\cos\alpha_{YK} = \frac{20(1-x)^2\alpha + 25(1-x^2)\beta}{16(1-x)^2\gamma + 25(1+x)^2\delta + 40(1-x^2)\epsilon}. \tag{2}$$

The molecular-field constants can be obtained from the observed variation of the saturation magnetization with zinc concentration. The exchange constants so obtained should be consistent with the existing data on similar ferrimagnetic systems. Detailed studies of the exchange interactions in magnetite by Smart[15] and Callen[16] have shown that J_{AB} obtained on the two-sublattice model is approximately -24 °K. The constants obtained on the two- and three-sublattice models are related through

$$J_{AB} = \tfrac{1}{9}(4J_\alpha + 5J_\beta).$$

From the theory of superexchange interactions the magnitude of both 180° d^5-O-d^5 and d^5-O-d^6 is large.[17] According to Callen,[16] $J_\alpha < J_\beta$; so we have assumed the following values: $J_\alpha = -21$ °K and $J_\beta = -28$ °K. From the data on lithium ferrite,[8] we have $\frac{1}{2}(J_\delta + J_{\delta'}) \sim -10$ °K. Assuming $ZnFe_2O_4$ to be antiferromagnetic[18] with $T_N = 15$ °K, a two-sublattice model calculation yields $|J_\delta| - |J_{\delta'}| \sim 0.5$ °K. Another calculation using the value -40 °K for the Curie-Weiss constant θ_p for[19] $ZnFe_2O_4$ yields the value of this difference between the exchange constants to be approximately 1 °K. We therefore take $J_\delta = -10$ °K and $J_{\delta'} = -11$ °K. Finally, we estimated the values of γ

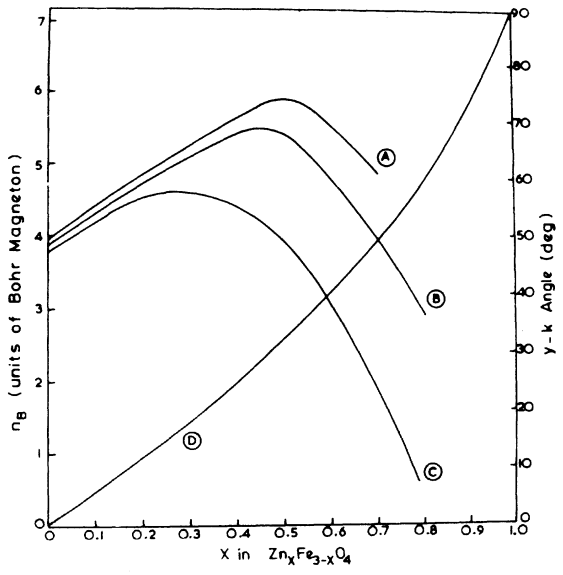

FIG. 5. Magneton number n_B (A, B, and C) and Yafet-Kittel angles (D) as a function of x in $Zn_xFe_{3-x}O_4$. A, Stuijts *et al.*, data at 5 °K; B, present data at 77 °K; C, present data at 303 °K.

and ϵ from the best fit for the variation of saturation magnetization with zinc concentration. Using the relation

$$n_B = (9+x)\cos\alpha_{YK} - 5(1-x)\,, \tag{3}$$

where n_B has been expressed in units of Bohr magneton, we obtain $J_\gamma = -64$ °K and $J_\epsilon = -24$ °K. As $J_\gamma \sim J_{\gamma'}$ and $J_\epsilon \sim J_{\epsilon'}$, we assume that the primed values are the same as the unprimed ones. The 90° Fe^{2+}-O-Fe^{2+} interaction is the largest. This is supported by the superexchange theory. The relative magnitudes of the exchange constants are in agreement[17] with the existing experimental data on other oxides.

It is now possible to understand to some extent the hitherto unexplained experimental observation of Stuijts *et al.*[4] in Zn substituted ferrites about the increase in magnetization with the increase in external magnetic field. In presence of the external magnetic field $\vec{H}_0$ the energy is given by

$$E = -\tfrac{1}{2}\sum_i \vec{m}_i\cdot\vec{H}_i - \sum_i \vec{m}_i\cdot\vec{H}_0\,. \tag{4}$$

Minimizing E yields the new equilibrium value of $\alpha_{YK}(H_0)$ which is given by

$$\cos\alpha_{YK}(H_0) = \cos\alpha_{YK}(0) - \frac{2H_0[(1-x)m_{B_1}(Fe^{2+}) + (1+x)m_{B_1}(Fe^{3+})]}{(N_A\mu_B d/M)^2[16(1-x^2)\gamma + 25(1+x)^2\delta + 40(1-x^2)\epsilon]}\,, \tag{5}$$

where $\alpha_{YK}(0)$ is the YK angle in absence of the external magnetic field. Reduction in the YK angle increases net magnetization. Calculations for $x = 0.7$ and $H_0 = 90$ kOe show that there would be 7% increase in the magnetization. This is small compared to the observed value of 15% change by Stuijts *et al.*[4] This discrepancy could be due to some transient effects in the measurement of magnetization on account of the pulsed fields employed or some errors in the absolute values of exchange and molecular-field constants used for the calculations.

C. Permeability spectrum

It is often convenient to consider the domains and the domain walls as entities and to analyze the permeability spectrum in terms of their dynamical response to external low- and high-frequency magnetic fields.[20] Vell-Coleiro *et al.*[21] have shown that this approach is applicable for the resonant motion of domain walls in yttrium-gadolinium-iron garnets. We briefly consider on these lines the response function of the magnetic system for rf excitations.

The usual equation of motion for domain walls is

$$m_w\ddot{z} + \beta_w\dot{z} + \alpha_w z = 2M_s H\,, \tag{6a}$$

where m_w is the effective mass per unit area of the domain wall, β_w is the damping constant, and α_w is the stiffness constant. A simple calculation shows that[11]

$$m_w = [2\pi\gamma_e^2\delta_w(1 + H_A/4\pi M_s)]^{-1} \tag{6b}$$

and

$$\alpha_w = 16\pi M_s^2/l(\mu_0 - 1)\,, \tag{6c}$$

where δ_w is the thickness of the wall, H_A is the anisotropy field, γ_e is the electronic gyromagnetic ratio, M_s is the saturation magnetization, μ_0 is the initial permeability, and l is the thickness of the domain.

The origin of the loss mechanism for domain-wall motion in ferrimagnetic materials is still not fully known.[22] In insulators these losses are assumed to arise from the coupling of the spins to lattice and to each other and hence should be given by the damping factor in the precessional motion of the magnetization. In this case[23]

$$\beta_w = 4\pi\lambda m_w\,, \tag{6d}$$

where λ is the Landau-Lifshitz damping constant.

For simplicity we consider only the 180° domain walls. From Eq. (6a), the contribution from domain-wall displacement to complex susceptibility at frequency ω is given by

$$\chi = \chi' - j\chi''\,, \tag{7a}$$

$$\chi' = \chi_0[1 - (\omega/\omega_0)^2]/[(1 - \omega^2/\omega_0^2)^2 + (\omega/\omega_c)^2]\,, \tag{7b}$$

$$\chi'' = \chi_0(\omega/\omega_c)/[(1 - \omega^2/\omega_0^2)^2 + (\omega/\omega_c)^2]\,, \tag{7c}$$

where

$$\omega_c = \alpha_w/\beta_w\,, \tag{7d}$$

$$\omega_0 = (\alpha_w/m_w)^{1/2}\,, \tag{7e}$$

and

$$\chi_0 = A M_s^2/\alpha_w\,. \tag{7f}$$

Here A is the area of the domain wall. The complex permeability is given by

$$\mu = \mu' - j\mu'' = (1 + 4\pi\chi') - j4\pi\chi''\,. \tag{7g}$$

For $\beta_w < 2(\alpha_w m_w)^{1/2}$, we obtain from Eq. (6a)

$$z = z_0 e^{-\Omega t}\sin(\omega_r t + \phi_0)\,, \tag{8a}$$

where ω_r and Ω are the resonance and relaxation frequencies respectively and ϕ_0 is an arbitrary phase constant. Here

$$\omega_r = (\omega_0^2 - \Omega^2)^{1/2} = (\alpha_w/m_w - \beta_w^2/4m_w^2)^{1/2} \quad (8b)$$

and

$$\Omega = \beta_w/2m_w \ . \quad (8c)$$

The probability for displacement of the domain wall from one equilibrium position to another is given[24] by $\omega_r e^{-U/kT}$, where U is the height of the potential barrier. For $\omega_0/\Omega \gg 1$, ω_r is large and the motion is free and undamped. On the other hand, for $\omega_0/\Omega \sim 1$, the motion is critically damped and as ω_r tends to zero, the domain wall remains bound to one position. For the intermediate case, say, $2 > \omega_0/\Omega > 1$, the domain wall is likely to execute damped oscillations at the position of equilibrium. From the study of the permeability spectrum, it is possible to estimate ω_0 and ω_c using Eqs. (7a)–(7f). The resonance and relaxation frequencies are then obtained from Eqs. (8b) and (8c), respectively. From these frequencies the response of the system to thermal and electromagnetic perturbations can be obtained.

If a 180° domain wall executes an oscillation at its equilibrium position a certain fraction p of atoms experiences spin-reversal periodically. We obtain p by a simple calculation. Since α_w is the force per unit area, the force on an atom is $\alpha_w a^2$, where a is the lattice constant. The average value of z^2 at temperature T, neglecting β_w, is

$$\langle z^2 \rangle = \left(\int_{-\infty}^{\infty} z^2 e^{-(\alpha_w a^2 z^2/2kT)}\, dz \right) \Big/ \int_{-\infty}^{\infty} e^{-(\alpha_w a^2 z^2/2kT)}\, dz = kT/\alpha_w a^2 .$$

Now as p is proportional to $2\langle z^2 \rangle^{1/2}/l$,

$$p = c(4kT/\alpha_w a^2 l^2)^{1/2} = (c/4\pi M_s a)[4\pi kT(\mu_0 - 1)/l]^{1/2} , \quad (9)$$

where c is a constant of order unity and depends on the nature of the domain wall. We will show in II that if p is not insignificant and the spin-reversal frequency is greater than the nuclear Larmor frequency, Mössbauer lines may have the characteristic features of a relaxed spectra.

We have considered so far the contribution from the domain-wall translation to the magnetic susceptibility. To include also the contribution from the domain rotation the susceptibility tensor with diagonal and off-diagonal elements has to be introduced.

Taking the simplest case of the uniaxial magnetic anisotropy, we obtain

$$\langle H_{an} \rangle = 2K_1/M , \quad (10)$$

where K_1 is the first-order anisotropy constant. In presence of an externally applied rf field of frequency ω, the contribution to the tensor susceptibility is readily obtained, and the diagonal element is given by[25]

$$\chi_{xx} = \chi'_{xx} - j\chi''_{xx} , \quad (11)$$

$$\chi'_{xx} = \frac{1}{4\pi} \frac{\omega_m \tau \omega_a \tau [(\omega_a \tau)^2 - (\omega\tau)^2 + 1]}{[(\omega_a \tau)^2 - (\omega\tau)^2 - 1]^2 + 4(\omega_a \tau)^2} , \quad (11a)$$

$$\chi''_{xx} = \frac{1}{4\pi} \frac{\omega_m \tau [(\omega_a \tau)^2 + (\omega\tau)^2 + 1]}{[(\omega_a \tau)^2 - (\omega\tau)^2 - 1]^2 + 4(\omega_a \tau)^2} , \quad (11b)$$

where $\omega_m = \gamma_e 4\pi M_s$, $\omega_a = \gamma_e \langle H_{an} \rangle$, and τ is the relaxation time for the domain rotation. The total susceptibility is given adding the contributions from domain translation [Eq. (9)] and domain rotation [Eq. (11)].

The results of the study of permeability spectrum are given in Fig. 3. These have been analyzed in terms of the domain displacement and rotation processes as discussed above. In Table III are given the observed resonance frequencies ω_0, ω_c, and Ω related to the domain oscillation. Also given are the calculated values of ω_a, the resonance frequency for the domain rotation. To obtain ω_a, use was made of the data on anisotropy constant obtained by Miyata.[3] Since ω_a was large compared to ω_0 in all cases, the dissipation part of the permeability spectrum in the region of dispersion was assumed to have contributions mainly from the domain wall displacement. In Fig. 6 is shown the computed curve for $Zn_{0.6}Fe_{2.4}O_4$ obtained from Eq. (7) using $\omega_0 = 20$ MHz and $\omega_c = 18$ MHz. The agreement with the experimental data is satisfactory. Similar agreement was observed in each case. The broad resonance just after the domain-wall resonance in Fe_3O_4 spectrum was identified as the dimensional resonance. The contribution to susceptibility from domain rotation was found to be small and this (within the range and accuracy of our measurement) could not be obtained precisely. There is, however, clear indication about its presence in the spectrum of $Zn_{0.4}Fe_{2.6}O_4$.

For $x = 0$ and 0.2 we find that $\omega_0/\Omega > 2$. For these cases the domain wall is expected to be relatively free and would move from one position to another under thermal excitation. On the other hand, for $x > 0.4$, ω_0/Ω lies between 2 and 1. For these cases we expect that the motion is damped and the domain wall would be bound to its equilib-

TABLE III. Observed characteristic frequencies (see text) for domain oscillations and the calculated resonance frequencies for domain rotation for $Zn_xFe_{3-x}O_4$. The values of anisotropy constant have been taken from Ref. 3.

	Domain oscillation						Domain rotation
x	ω_0 (MHz)	ω_c (MHz)	Ω (MHz)	$\frac{\omega_0}{\Omega}$	10^4K_1 (erg/cm^3)	$\frac{2K_1}{M}$ (Oe)	ω_a (MHz) Calc.
0.0	30	60	7.5	4	14	640.7	1790
0.2	30	75	6	5	8	302.5	845
0.4	50	50	25	2	2.5	102.0	285
0.6	20	18	11	1.8	1.0	56.3	155
0.8	40	20	40	1	0.1	62.0	175

rium position. As discussed in II thermal excitations of these oscillations will change the shape of the Mössbauer lines significantly. This has been observed in the Mössbauer spectra of these samples and is reported in II. The permeability data therefore helps here to account for the observed change in the Mössbauer line shape as the zinc concentration is varied in $Zn_xFe_{3-x}O_4$.

From Eqs. (6c) and (8b) the relaxation frequency Ω is directly proportional to λ. If the main contribution to λ comes from the anisotropy field, it would approximately vary linearly[26] as K_1^2/M_s^3. This has not been observed. It then follows that contributions from other sources should also be considered. Alternately, it may also happen that λ for the process of domain translation may not be the same as the one obtained by the conventional resonance experiment. More observations are required to resolve this issue.

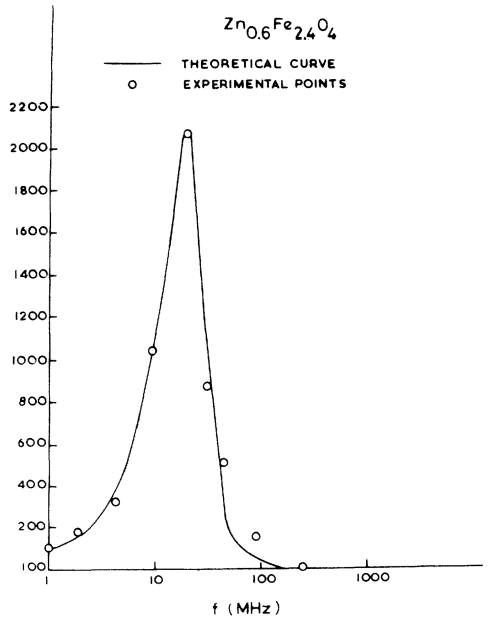

FIG. 6. Computed permeability spectrum (dissipative part), for $Zn_{0.6}Fe_{2.4}O_4$ with $\omega_0 = 20$ MHz and $\omega_c = 18$ MHz [see text, Eqs. (7c) and (7g)].

IV. CONCLUSION

The $Zn_xFe_{3-x}O_4$ ferrites were prepared in pellet form using a low oxygen partial pressure technique. The observed variation of the saturation magnetization with zinc concentration has been explained on the basis of the existence of Yafet-Kittel angles on the B site spins. Using a three sublattice model, exchange constants have been obtained in the molecular-field approximation. The values of these exchange integrals have been shown to be in broad agreement with the present theory of superexchange interactions as well as estimates made from other experiments.

The existence of magnetic relaxation effects in the permeability spectrum has been explained satisfactorily on the basis of domain wall oscillation and domain rotation processes. As zinc concentration was increased, the relaxation frequency increased with respect to the resonance frequency. Our analysis indicates that for domain translation, in addition to the random fluctuations of the anisotropy field, other unknown relaxation processes are also present.

ACKNOWLEDGMENTS

We are grateful to Dr. M. J. Patni for a series of helpful discussions during the preparation of the paper. One of us (R.G.S.) is grateful to the Government of Madhya Pradesh and Government of India, Ministry of Education, for a grant under Quality Improvement Programme, which made his participation possible in this study. Another (N.G.N.) would like to acknowledge the financial support received from the Council of Scientific and Industrial Research, Government of India, during the period of this study.

[1]C. Guillaud, J. Phys. Radium 12, 239 (1951).
[2]E. W. Gorter, Phillips Res. Rep. 9, 321 (1954).
[3]N. Miyata, J. Phys. Soc. Jpn. 16, 1291 (1961).
[4]A. L. Stuijts, D. Veeneman, and A. Broese van Groenon, in *Ferrites*, edited by Y. Hoshino, S. Iida, and M. Sugimoto (University Park, Tokyo, 1971), p. 236.
[5]D. C. Dobson, J. W. Linnett, and M. M. Rehman, J. Phys. Chem. Solids 31, 2727 (1970).
[6]C. M. Srivastava, S. N. Shringi, and R. G. Srivastava, following paper, Phys. Rev. B 14, 2041 (1976), hereafter referred to as II.
[7]N. S. Satya Murthy, M. G. Natera, S. I. Youssef, R. J. Begum, and C. M. Srivastava, Phys. Rev. 181, 969 (1969).
[8]J. W. Young and J. Smit, J. Appl. Phys. 42, 2344 (1971).
[9]S. C. Bhargava and P. K. Iyengar, Phys. Status Solidi B46, 117 (1971); 53, 359 (1972).
[10]J. M. Daniels and A. Rosencwaig, Can. J. Phys. 48, 381 (1970); and P. Raj and S. K. Kulshreshtha, Phys. Status Solidi A 4, 501 (1971).
[11]J. Smit and H. P.J . Wijn, *Ferrites* (Wiley, New York, 1959).
[12]M. A. Gilleo, J. Phys. Chem. Solids 13, 33 (1960).
[13]L. K. Leung, B. J. Evans, and A. H. Morrish, Phys. Rev. B 8, 29 (1973).
[14]C. M. Srivastava and M. J. Patni, J. Magn. Res. 15, 359 (1974).
[15]J. S. Smart, in *Magnetism*, edited by G. T. Rado and H. Suhl (Academic, New York, 1963), Vol. III, p. 63.
[16]E. Callen, Phys. Rev. 150, 367 (1966).
[17]J. B. Goodenough, *Magnetism and the Chemical Bond* (Wiley, New York, 1963), p. 168.
[18]F. K. Lotgering, J. Phys. Chem. Solids 27, 139 (1966).
[19]P. K. Baltzer, P. J. Wojtowicz, M. Robbins, and E. Lopatin, Phys. Rev. 151, 367 (1966).
[20]C. Kittel and J. K. Galt, in *Solid State Physics*, edited by F. Seitz and D. Turnbull (Academic, New York, 1956), Vol. III, p. 437. Also, G. A. Kraftmakher, V. V. Meriakni, A. Ya. Chervonenkis, and V. I. Shcheglov, Zh. Eksp. Teor. Fiz. 63, 1353 (1972) [Sov. Phys.-JETP 36, 714 (1973)].
[21]G. P. Vell-Coleiro, D. H. Smith, and L. G. Van Uitert, J. Appl. Phys. 43, 2428 (1972).
[22]J. F. Dillon, Jr., in *Magnetism*, edited by G. T. Rado and H. Suhl (Academic, New York, 1963), Vol. III, p. 415. Also, C. E. Patton, IEEE Trans. Magn. MAG-9, 559 (1973), and references therein.
[23]R. F. Soohoo, *Magnetic Thin Films* (Harper and Row, New York, 1965), p. 176.
[24]P. Gaunt, IEEE Trans. Magn. MAG-9, 171 (1973).
[25]B. Lax and K. J. Button, *Microwave Ferrites and Ferrimagnetics* (McGraw-Hill, New York, 1962), p. 154.
[26]M. Sparks, J. Appl. Phys., 36, 1670, (1965); P. E. Seiden and M. Sparks, Phys. Rev. 137, A1278 (1965); R. Krishnan, IEEE Trans. Magn. MAG-6, 618 (1970).